International Journal for Rapid Research in Engineering Technology & Applied Science
Vol VIII Issue VIII Aug 2022
ISSN Online: (2455-4723)

Performance Analysis of V2G and G2V System with Hybrid Renewable Energy Sources

M.tech. Scholar Surendra Kumar Chourasiya, Professor. Vinay Pathak
Electrical & Electronics Engineering, Bhopal Institute of Technology, Bhopal (M.P.) (M.P) INDIA
surendrachourasiya01@gmail.com, pathakvinay2000@gmail.com

ABSTRACT: Wind power is one of the most developed and rapidly growing renewable energy sources. The thesis is dedicated to an in-depth analysis of DFIG PV and wind energy generators, system configurations, power converters, control schemes and dynamic and steady state performance of practical wind energy conversion systems (WECS). This thesis focuses on method for controlling the DC link voltage and maximum power point tracking (MPPT) of the photovoltaic (PV) system in a hybrid PV-wind turbine system is introduced. The system under study is a modified PV-DFIG structure. In this system, the PV output power is injected into the grid through the both grid-side and rotor-side converters of the DFIG. The proposed control system controls the DC-link voltage and the MPPT of the PV system together. This system is economically justifiable given to the elimination of the PV dedicated converter and can inject the PV output power into the grid more efficiently. The results are simulated in the MATLAB/SIMULINK software environment. The dynamic model is developed using the machines equivalent circuit and is expressed in the stationary, rotor and the synchronous reference frames for evaluating the performance of the machine. The stator of the DFIG is directly interfaced to the grid and by controlling the rotor voltage by a two-level back-to-back converter the grid synchronization and power control is maintained. The Grid Side Converter (GSC) is modified for feeding regulated power to the grid. Rotor Side Converter (RSC) is controlled for achieving MPPT and Unity Power Factor (UPF) and with and without PV system Both Simulation done in MATLAB and Voltage, Current, real and reactive power for input and output Result carried.

Keywords V2G and G2V three -phase inverter, MPPT, BSS, solar, DFIG

I INTRODUCTION

Renewable energy is power derived from natural possessions, such as solar, wind, waves, or geothermal energy. These resources are renewable and can be recycled naturally. Therefore, compared to the depletion of traditional fossil fuels [1], these sources of information are considered inexhaustible. The global power crunch provides a new impetus for the development or maturity of clean or renewable energy. [2]. In addition to the decline in fossil fuel transportation worldwide, another major reason fossil fuels do not work is the pollution associated with burning fossil fuels. In contrast, it is well known that compared to traditional energy sources, renewable energy sources are cleaner, or energy produced has no adverse effects on pollution.

Correspondingly, the solar power generation system is proposed in Figure 1.2. A solar cell or panel comprises a model derived from solar cells connected in series or parallel to provide the required currents and energy. solar intertie photovoltaic (PV) systems are not particularly complex. First there are panels, which collect the sunlight and turn it into electricity. The DC signals are fed into an inverter, which converts the DC into grid-compatible AC power (which is what you use in your home). Various switch boxes are included for safety reasons, and the whole thing is connected via wires and conduit.

Storage batteries can provide protective power during periods of free sunlight by storing more or part of the power from solar panels. Solar power generation systems are used for private power consumption, weather stations, radio or television stations, entertainment venues, such as cinemas, hotels, restaurants, villages, and islands. The traditional p-n junction solar cell is the most advanced solar energy collection technology. The fundamental physics of energy input and carrier output functions the physical properties and the associated electrical properties (i.e., the band distance). The electron needs to have energy greater than the band gap to excite electrons from the valence band to the conduction band. An ideal solar cell has a direct band gap of 1.4 eV to absorb the maximum number of photons from the sun's radiation. The seemingly infinite lattice creates bands of allowed energy states; silicon creates a band gap where no electrons exist (a band gap that is 1.1 eV wide. However, the sun's radius is close to the black spectrum of about 6000 K. Therefore, most of the rays from the sun reaching the earth have a source of energy greater than the radius of the sun silicon group. These high-energy phonons will be cured by solar cells. Still, the distance between the phonons and the silicon band will be converted to heat (via an overflow called phonons) instead of usable energy. For a single meeting

cell, this will set a maximum efficiency of around 20%. Current research methods to perform multi-node photovoltaic design to overcome efficiency limits do not seem to be an expensive solution. Even a built-in PV device can only be used during the day and needs direct sunlight (directly connected to the interior) for optimum performance.

The major components of a wind turbine system are shown in Figure 1.9 (drawing not to scale). The turbine is formed by the blades, the rotor hub and the connecting components. The drive train is formed by the turbine rotating mass, low-speed shaft, gearbox, high-speed shaft, and generator rotating mass. It transfers turbine mechanical output power up to the generator rotor where it is converted to electrical power. The wind strikes the rotor on the horizontal-axis turbine, causing it to spin. The low-speed shaft transfers energy to the gear box, which steps up in speed and rotates the high-speed shaft. The high-speed shaft causes the generator to spin, hence generating electricity. The yaw system is used to turn the nacelle so that the rotor faces into the wind. The low-speed Shaft contains pipes for the hydraulics system that operates the aerodynamic brake. The high-speed shaft is equipped with an emergency mechanical brake which is used in case of failure of the aerodynamic brake [12].

The generator converts mechanical power of wind into electrical power. Usually, the generator produces power at low voltage and the transformer steps up the generator output voltage to connected grid voltage. The transformer may be placed at the bottom of the tower [4] or in the nacelle for losses minimization [13].

Other components of wind turbine system are the anemometer to measure wind speed and a wind vane which measure the wind direction. Wind speed information is used to determine when the wind speed is sufficient to start up the turbine and when, due to high winds, the turbine must be shut down for safety whereas wind direction measurement is used by the yaw-control mechanism which helps in orienting the rotor to the wind direction [14]. Electric fans and oil coolers are used to cool the gearbox and generator.

II RELATED WORK

Youssef Moumani et al. (2021) discusses the modelling and control of WECS' DFIG (Doublely-Fed Induction Generator) (Wind Energy Conversion System). The RSC (Rotor Side Converter) is controlled via a Non-Linear control approach based on backstepping. The final objective is to extract as much power as possible from WT (Wind Turbine). This is accomplished by regulating the active and reactive power of the DFIG independently. To evaluate and simulate the performance of this control approach, the Matlab/Simulink software environment was used. As a result, the system's performance is measured in terms of its capacity to endure random variations in wind speed and other parametric irregularities. In terms of overall performance, simulations show that this technology beats more typical linear controllers.

Abdeslam Jabal Laafou et al. (2020) DFIG (Double-Fed Induction Machine) used in the WECS is simulated and operated (Wind Energy Conversion System). In this paper, two PI controllers are proposed. The RSC (Rotor Side Converter) is used to adjust the WT for best power extraction from a wind turbine (Wind Turbine). Using the second way, a GSC (Grid Side Converter) is employed to keep the DC bus voltage constant. We added wind speed to the DFIG to help us comprehend the distinctions between hyper-synchronous and hypo-synchronous modes. The proposed control was designed and simulated using the Matlab/Simulink software environment to ensure its efficacy.

III PROPOSED SYSTEM

The grid-interfaced DFIG-based WECS is proposed for power smoothing in this paper. For rotor position estimation, the rotor position computation method is utilised [24]. The work's uniqueness comes from GSC's control (Grid Side Converter). The control algorithm for providing regulated electricity to the grid has therefore been explicitly proven by the authors. Another essential feature of DFIG-based WECS for power smoothening is BESS selection. When comparing the standard DFIG with the suggested DFIG, the differences in powers with increasing wind speeds are displayed. The system's functioning has been experimentally confirmed for controlling DFIG power under fluctuating wind speed circumstances. The Simulink design in this proposed DFIG system with solar and without solar.

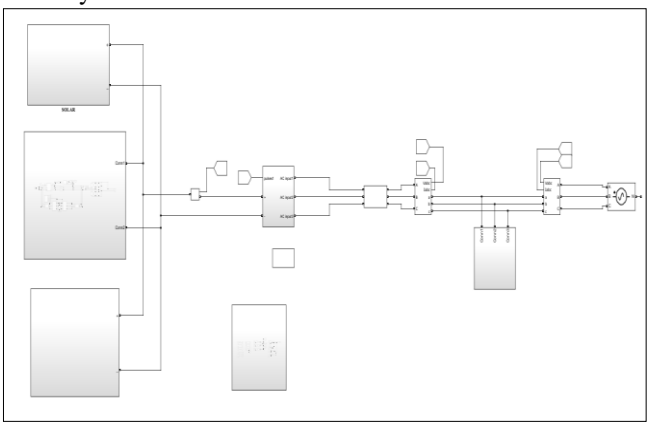

Figure 1: Proposed Simulink Model

This work proposes the grid interfaced DFIG based WECS for power smoothening. The rotor position computation

algorithm is used for the estimation of rotor position [24]. The novelty of the work lies in the control of GSC (Grid Side Converter). So, the authors have clearly demonstrated the control algorithm for feeding regulated power to the grid. The selection of BESS is the other important aspect of DFIG based WECS for power smoothening. The variations in the powers with the increase in wind speeds are demonstrated by comparing the conventional DFIG and the proposed DFIG. The operation of the system is experimentally validated for regulating the power of DFIG even under variable wind speed conditions.

1. **MATLAB Simulation without Solar:** Figure 1 shows a schematic representation of the proposed grid interfaced DFIG based WECS. The BESS is linked to the DC connection of two VSCs that are connected back-to-back. The stator is directly linked to the grid in this case. In a voltage-oriented reference frame, RSC is regulated. EPLL is used to align the d-axis of the synchronously rotating reference frame with the voltage axis (Enhanced Phase Locked Loop). The rotor position computation technique is utilised to estimate the location here. The GSC is set up such that the regulated electricity is supplied into the grid. When the generated power exceeds the regulated power, the leftover energy is stored in the BESS. If the amount of energy generated is less than the regulated amount, the BESS feeds the leftover energy to the grid. Figure 2 depicts the control algorithms.

Doubly Fed Induction Generator Based Wind Energy Systems: Doubly-fed electric machines are basically electric machines that are fed ac currents into both the stator and the rotor windings. Most of the doubly-fed Induction machines used in industry are of wound rotor type. Doubly-fed induction machines have found great use in today's wind power generation industry.

Doubly-fed induction generators (DFIGs) are by far the most widely used type of doubly- fed electric machine, and are one of the most common types of generators used to produce electricity in wind turbines because of the numerous advantages over other types of generators when used in wind turbine technology. The primary advantage of doubly-fed induction generators when used in wind turbines is that they allow the amplitude and frequency of their output voltages to be maintained at a constant value, regardless of the wind speed. Because of this, doubly-fed induction generators can be directly connected to the ac power network without the use of bulky and costly power converters and remain synchronized at all times with the ac power network. Other advantages include the ability to control the power factor (e.g., to maintain the PF at unity), while keeping the power electronics devices in the wind turbine at a moderate size.

The larger the battery, the more reliable it is, but it also raises the initial outlay. However, the battery's low rating has an impact on its dependability. As a result, suitable BESS design is required for the proposed WECS to function properly. The BESS's storage capacity is determined by the site's estimated wind profile. The total energy stored in the battery determines the BESS's rating. The constant value of the power feeding to the grid in this proposed DFIG is chosen as the average value of the power generated from prior wind data. When the power produced by the DFIG exceeds the regulated power, the energy held in the BESS is released. When the power production is less than the regulated power, however, the energy is absorbed from the BESS. The average power is calculated using historical wind data from a specific wind location. For the most common battery types, a generic battery model is implemented. For Lithium-Ion batteries, temperature and age (due to cycling) effects may be set.

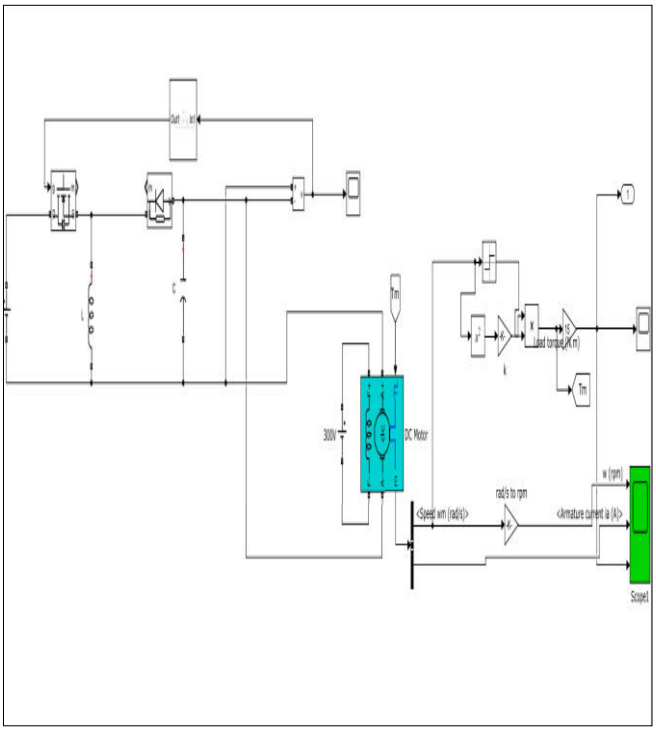

Figure 2: DC machine

Implements a (wound-field or permanent magnet) DC machine. For the wound-field DC machine, access is provided to the field connections so that the machine can be used as a separately excited, shunt-connected or a series-connected DC machine.

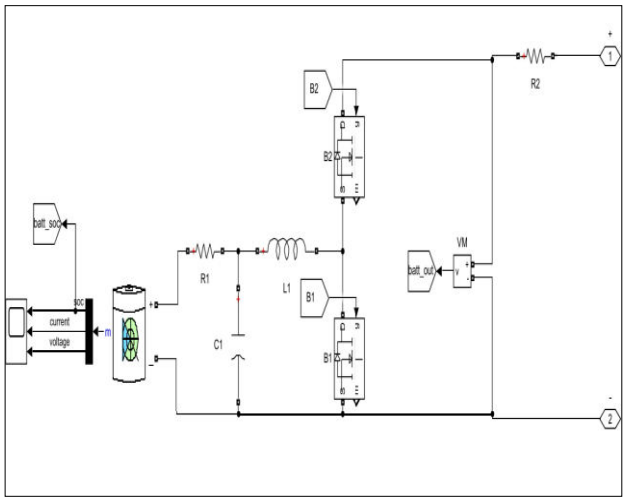

Figure 3: Battery Simulink Model

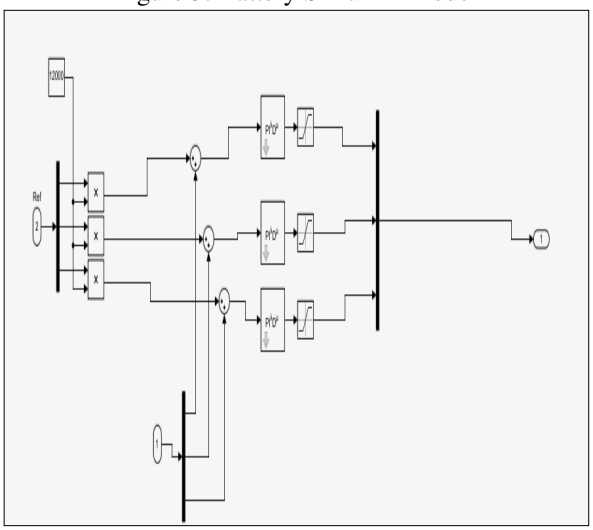

Figure 4: Fractional PID

MATLAB IMPLEMENTATION WITH SOLAR:

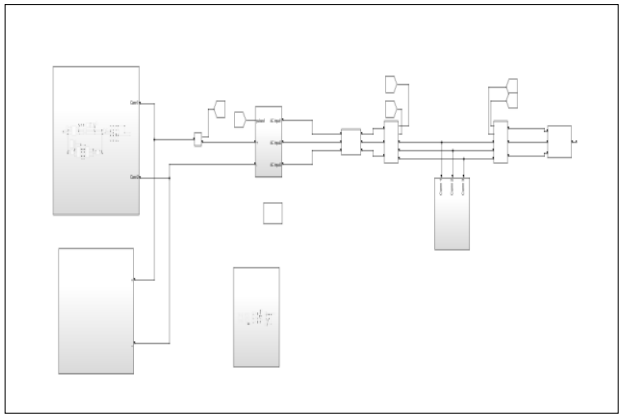

Figure 5 Proposed Simulink Model with Solar Panel

SOLAR -This block models a solar cell as a parallel combination of a current source, two exponential diodes and a parallel resistor, Rp, that are connected in series with a resistance Rs. The output current I is given by:

- I = Iph - Is*(e^((V+I*Rs)/(N*Vt))-1) - Is2*(e^((V+I*Rs)/(N2*Vt))-1) - (V+I*Rs)/Rp

where Is and Is2 are the diode saturation currents, Vt is the thermal voltage, N and N2 are the quality factors (diode emission coefficients) and Iph is the solar-generated current. Models of reduced complexity can be specified in the mask. The quality factor varies for amorphous cells, and typically has a value in the range of 1 to 2. The PS input Ir is the irradiance (light intensity) in W/m^2 falling on the cell. The solar-generated current Iph is given by Ir*(Iph0/Ir0) where Iph0 is the measured solar-generated current for irradiance Ir0.

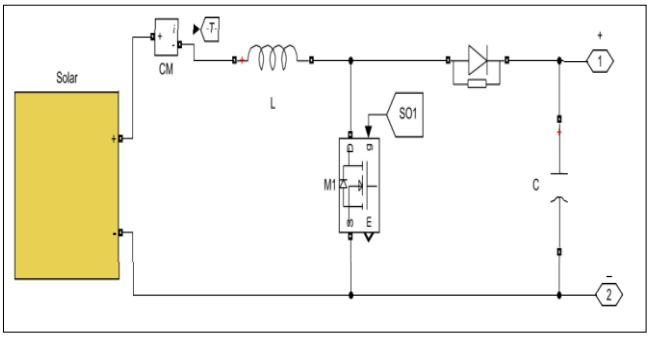

Figure 6: Solar System

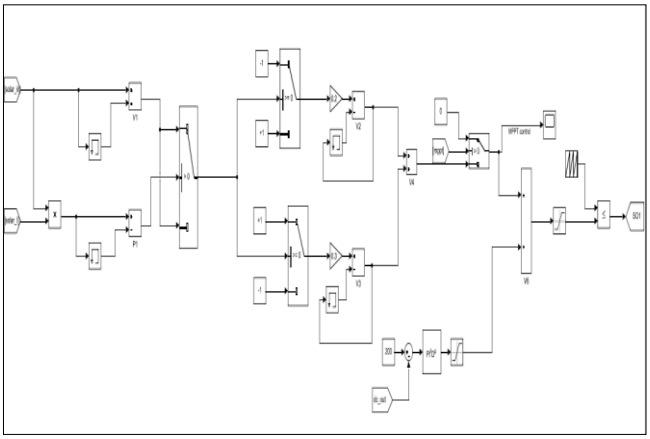

Figure 7: MPPT Control

The larger the battery, the more reliable it is, but it also raises the initial outlay. However, the battery's low rating has an impact on its dependability [18]. As a result, suitable BESS design is required for the proposed WECS to function properly. The BESS's storage capacity is

determined by the site's estimated wind profile. The total energy stored in the battery determines the BESS's rating.

Table 1: DC Machine

Parameter	Value
Armature resistance and inductance [Ra (ohms) La (H)]	2.581 0.028
ield resistance and inductance [Rf (ohms) Lf (H)]	281.3 156
Field-armature mutual inductance Laf (H):	0.9483
Total inertia J (kg.m^2)	0.02215
Viscous friction coefficient Bm (N.m.s)	0.002953
Coulomb friction torque Tf (N.m)	0.5161
Initial speed (rad/s) :	0.001
Initial field current:	1.06647707074298

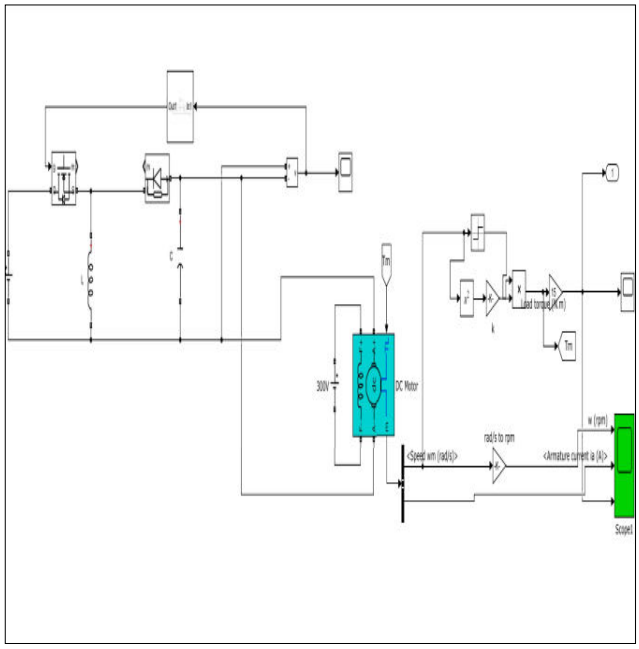

Figure 7: Dc Machine

Implements a (wound-field or permanent magnet) DC machine for the wound-field DC machine, access is provided to the field connections so that the machine can be used as a separately excited, shunt-connected or a series-connected DC machine.

Three-phase asynchronous machine -Implements a three-phase asynchronous machine (wound rotor, squirrel cage or double squirrel cage) modelled in a selectable dq reference frame (rotor, stator, or synchronous). Stator and rotor windings are connected in wye to an internal neutral point

Table 2: Three-Phase Asynchronous Machine

Parameter	Value
Nominal power, voltage (line-line), and frequency [Pn(VA),Vn(Vrms),fn(Hz)]:	[60e3 450 50]
Stator resistance and inductance [Rs,Lls] (pu):	[0.21 2.43e-3]
Rotor resistance and inductance [Rr',Llr'] (pu):	[0.22 2.43e-3]
Mutual inductance Lm (pu):	
Inertia constant, friction factor, pole pairs [H(s) F(pu) p()]:	
[slip, th(deg), ia,ib,ic(pu), pha,phb,phc(deg), iar,ibr,icr(pu), phar,phbr,phcr(deg)]:	

The constant value of the power feeding to the grid in this proposed DFIG is chosen as the average value of the power generated from prior wind data. When the power produced by the DFIG exceeds the regulated power, the energy held in the BESS is released. When the power production is less than the regulated power, however, the energy is absorbed from the BESS. The average power is calculated using historical wind data from a specific wind location. For the most common battery types, a generic battery model is implemented. For Lithium-Ion batteries, temperature and age (due to cycling) effects may be set.

Table 3: FOPID Parameters

Parameter	Value
Kp	1.2
Ki	1
lambda	0.5
Kd	0.05
mu	0.5
Frequency range [wb, wh]	[0.001, 1000]
Approximation order	5

Fractional PID with parameters Kp, Ki, Kd and extended parameters lambda and delta:

PI^{lambda}D^{mu} = Kp + Ki*s^-{lambda} + Kd*s^{mu}

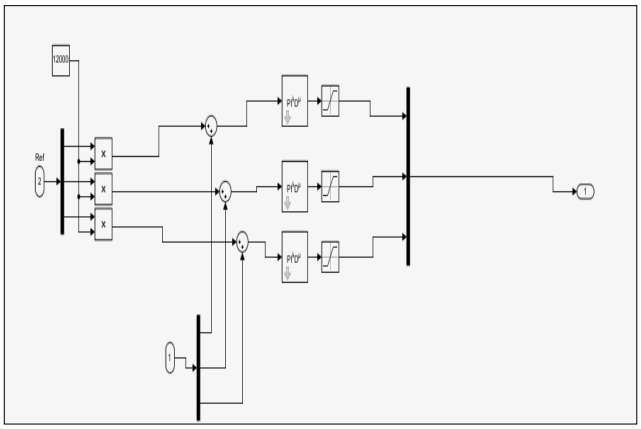

Figure 8: Fractional PID

Fopid Fractional PID with parameters Kp, Ki, Kd and extended parameters lambda and delta: PI^{lambda}D^{mu} = Kp + Ki*s^-{lambda} + Kd*s^{mu}

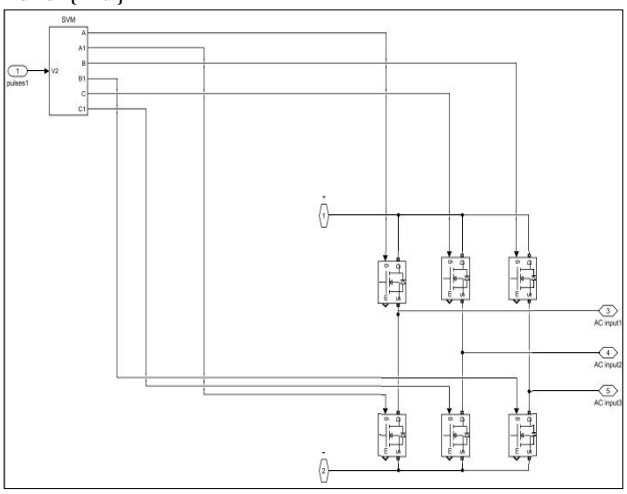

Figure 9: SVM Subsystem

IV SIMULATION RESULT

The parameters of the PV panel, wind turbine and DFIG,. Simulation is done on MATLAB 2019b and results shown below. Generated voltage of solar PV system is not sufficient since a boost converter is used for rise of voltage.A detailed electromechanical model of a DFIG-based wind turbine connected to power grid as well as autonomously operated wind turbine system with integrated battery energy storage is developed in the MATLAB/Simulink environment and its corresponding generator and turbine control structure is implemented. A thorough explanation of this control structure as well as the steady state behavior of the overall wind turbine system is presented. The steady state reactive power capability of the DFIG.

SIMULATION RESULT WITHOUT SOLAR AND DFIG:

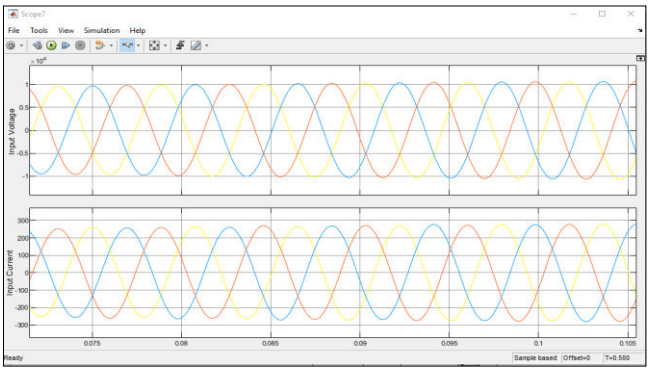

Figure 10: Input Voltage and Current

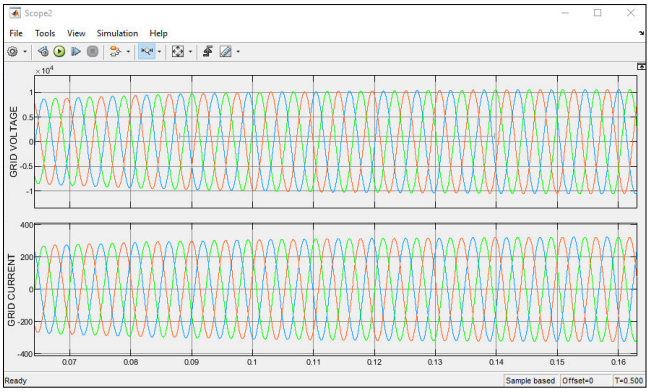

Figure 11: Grid Voltage and Current

Figure 11 showing the Grid Voltage and Current waveform, during simulation grid voltage generate 230v

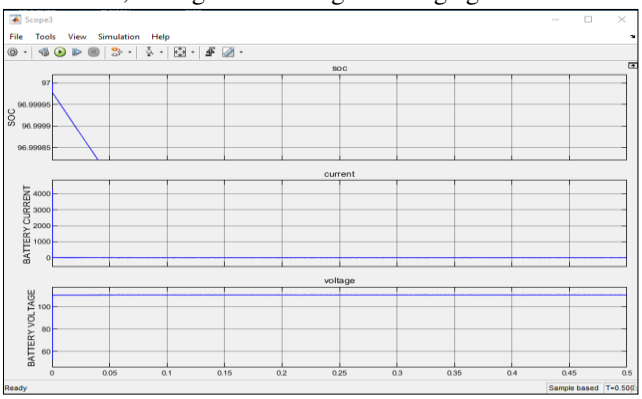

Figure12:BatteryOutput

Figure 12 Battery Output showing with soc and battery voltage and current waveform ,battery charge upto 97 % at discharge after 97%, State of charge (SoC) is **the level of charge of an electric battery relative to its capacity**. The units of SoC are percentage points (0% = empty; 100% = full).

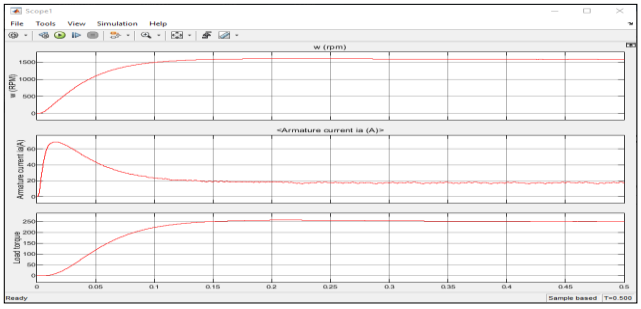

Figure 13: DC Machine Output

Figure 13: DC Machine Output rpm, armature current and load voltage , he stator consists of field windings while the rotor (also called the armature) consists of an armature winding. When both the armature and the field windings are excited by a DC supply, current flows through the windings and a magnetic flux proportional to the current is produced

f

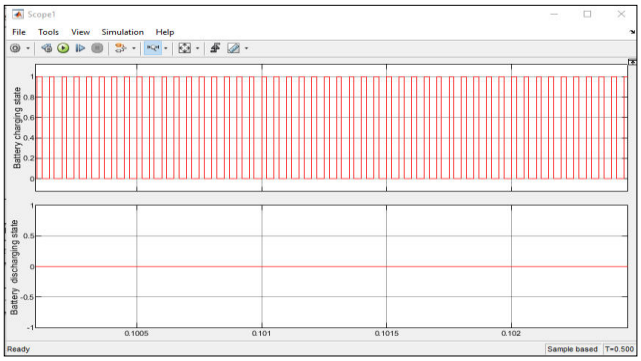

Figure14: Battery Charging and Discharging States

Figure 14 showing the Battery Charging and Discharging States ,battery discharge at 0% and charging at 100%, The direction of current through the battery determines whether it is charging or discharging. The battery is trying to push current in a particular direction. If the current flows in that direction, the battery is discharging. If the current flows in the other direction, the battery is charging

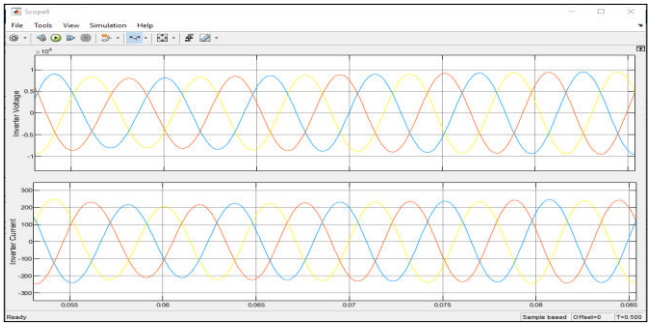

Figure 15: Inverter Current and Voltage

Figure 15 showing the three phase Inverter Current and Voltage, A three-phase inverter converts a DC input into a three-phase AC output. Its three arms are normally delayed by an angle of 120° so as to generate three-phase AC supply. The inverter switches each has a ratio of 50%

SIMULATION RESULT WITH SOLAR AND DFIG:

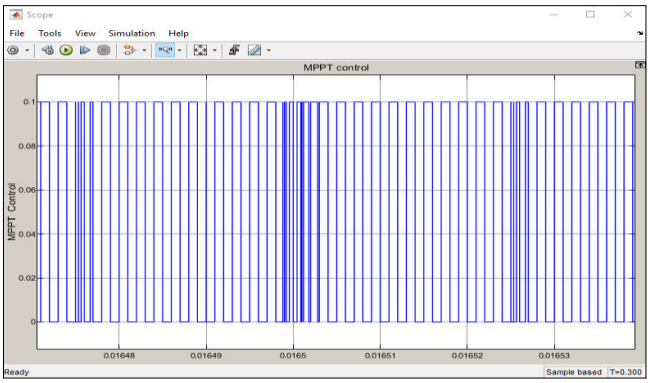

Figure 16: MPPT Control

the maximum power point tracker is an electronic DC to DC converter that optimizes the match between the solar array (PV panels), and the battery bank or utility grid.

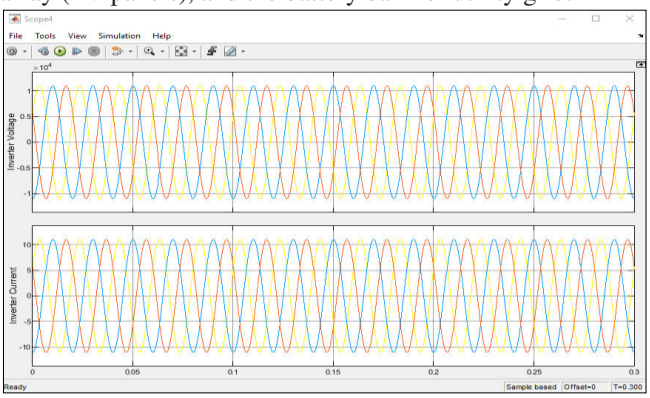

Figure 17: Input Voltage and Current

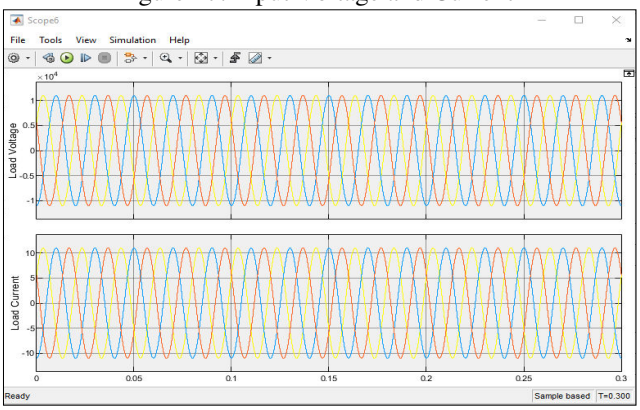

Figure 18: Load Voltage and Current

The amount of current" drawn by the thing that is connected to the output of the circuit. The actual power supply voltage that can be used when switching a load or continuously in an OFF state. The actual power supply voltage that can be used when switching a load or continuously in an OFF state.

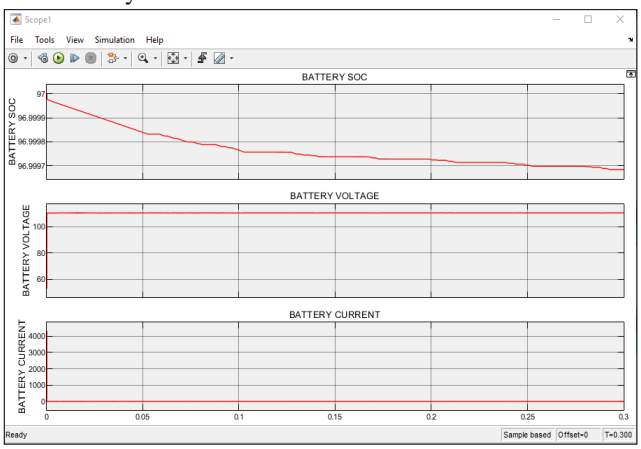

Figure 19: Battery Output

Fig 19 showing the battery output ,Power capacity is how much energy is stored in the battery.

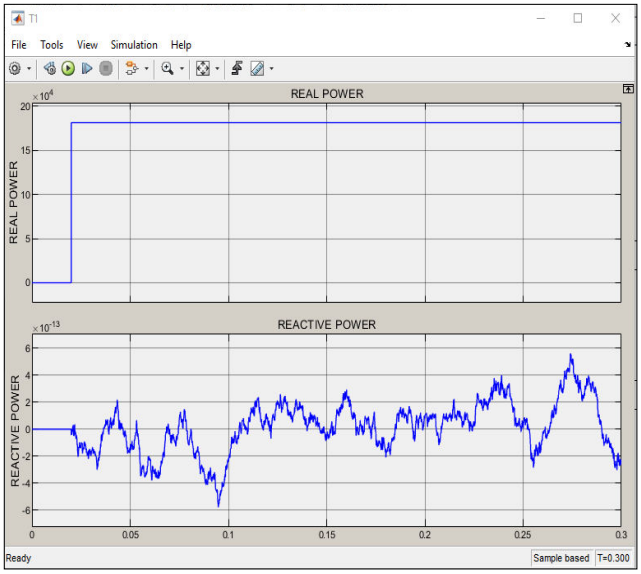

Figure 20: Real Power and Reactive Power

The active power is the real power consumes by the load. Whereas, the reactive power is the useless power. The active power is the product of the voltage, current and the cosine of the angle between them. Whereas, the reactive power is the product of voltage and current and the sine of the angle between them.

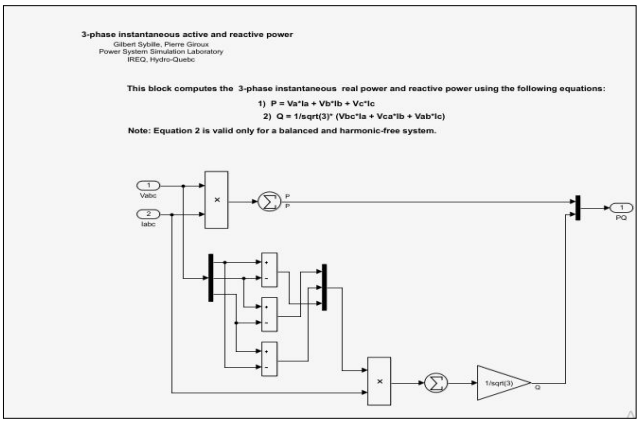

Figure 21: Phase Instantaneous Active and Reactive Power

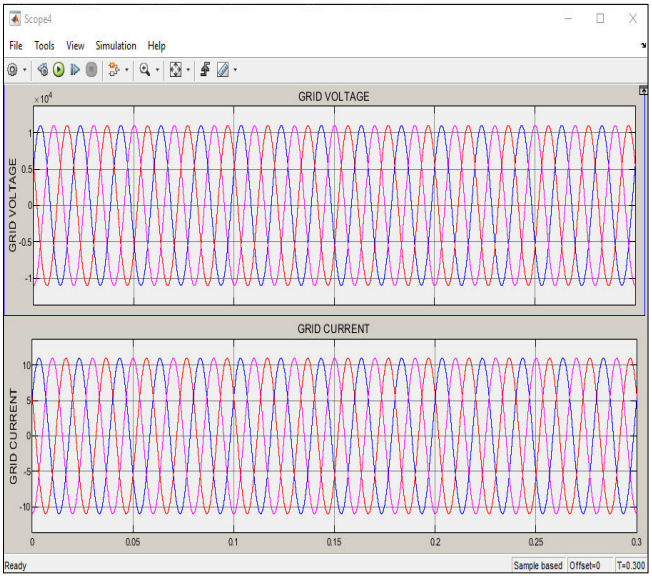

Figure 22: Grid Voltage and Current

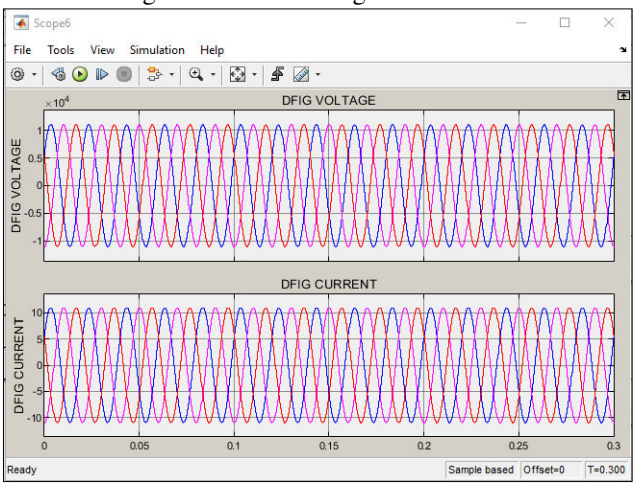

Figure 23: DFIG Voltage and Current

The DFIG consists of a 3 phase wound rotor and a 3 phase wound stator. The rotor is fed with a 3 phase AC signal which induces an ac current in the rotor windings.

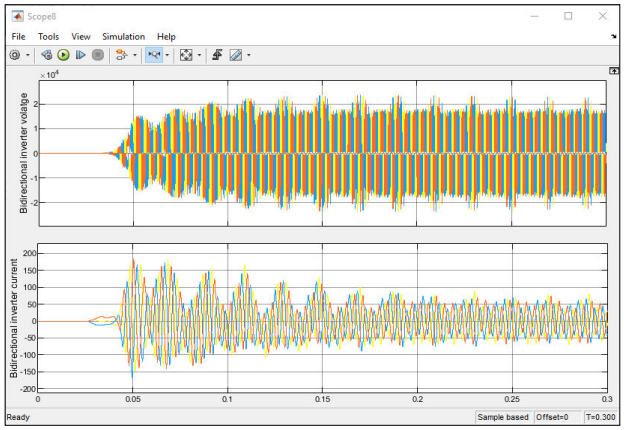

Figure 24: Bidirectional Inverter Current and Voltage

The bidirectional DC-AC inverter transfers power from the DC stage to the connected AC grid while the DC loading requirement is small. Or, the inverter transfers the power from the connected AC grid to the DC stage if the DC energy is insufficient for the DC loading requirement.

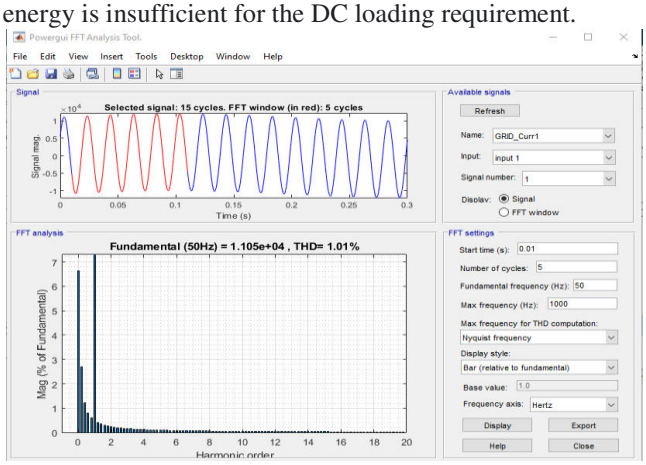

Figure 25 with solar thd

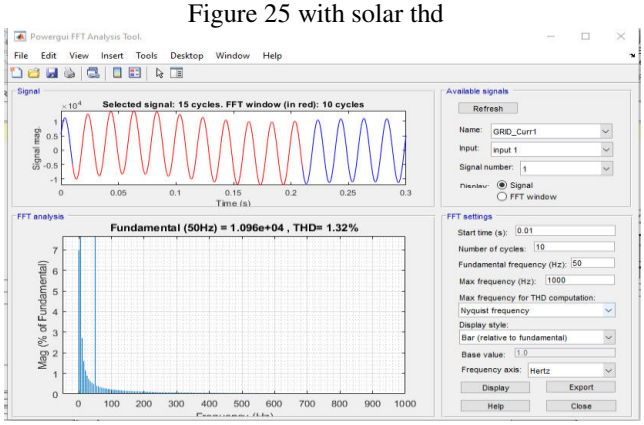

Figure 26 Without solar THD

Table 3 showing the comparison result in between proposed wok and exiting work, solar irradiance and grid power compare with the existing work, in the proposed work grid power showing higher as compare to existing work

Table 3 Power comparison with existing work

	Technique	Solar Irradiance	Grid power
Proposed system	MPPT,P& O	1000 rad/S	20 KW
Existing system	Predictive MPPT	1000 rad/S	15 W

Table 4 THD comparison With Solar and without solar

MODEL	THD
With Solar	**1.01**
Without Solar	**1.32**

Table 4 Showing The THD Comparison With And Without Solar, In The Proposed System Two Model Designed As DFIG With Solar And DFIG Without Solar, With Solar THD Showing Better As Compare To Without Solar

V CONCLUSION

Conclusions A new methodology for controlling the frequency of a microgrid through DFIG was proposed in this paper. The droop control implemented in the GSC together with the BESS connected in the DC link of the back-to-back converter of the DFIG, succeeded in successfully regulating the frequency of the microgrid at the moment of the disturbance. Implementing the droop control in the GSC of DFIG allowed the wind turbine to operate at all times at the point of maximum power extraction, while the power required for frequency control was provided by BESS. From the point of view of frequency control, the droop control showed great results in both super-synchronous and sub-synchronous operation, decreasing the accommodation times and the frequency nadir when compared to the frequency of the microgrid without DFIG intervention. On the other hand, when using BESS, the wind system can become more efficient because when DFIG operates connected to the network and in super-synchronous mode, the battery can be charged while BESS keeps the DC link voltage controlled, in order to maintain stored power to assist in frequency regulation.

Finally, for sub-synchronous operation, BESS controls the voltage of the DC link by discharging the battery.

The global energy consumption is increasing and the wind power generation is steadily rising and is being seen as a supplement and an effective alternative to large conventional power generation units. The power generated from wind energy systems needs to be fed into the grid and hence there is a need of an efficient interface between the wind energy systems and the grid. Power electronics serves as interface is necessary not only for the renewable energy source but also for its effects on the power system operation as the wind energy systems serve as an intermittent source of energy. The power electronics technology plays a very important role in the integration of renewable energy sources into the electrical grid, and it is widely used and rapidly expanding as these applications become more integrated with the grid systems. The technology used in the early developed wind turbines was based on a squirrel cage induction generator (SCIG) connected directly to the grid. This almost transfers the wind power pulsations to the electrical grid. There was no control of active and reactive powers which are key parameters to control frequency and voltage. This thesis, after conducting extensive literature review, explains how controlled active power, according to the grid requirements can be fed into the system.

VI REFERENCES

1. Youssef Baala, Seddik Bri DFIG-Based Wind Turbine Control Using High-Gain Observer 2020 1st International Conference on Innovative Research in Applied Science, Engineering and Technology (IRASET) Year: 2020 | Conference Paper | Publisher: IEEE DOI: 10.1109/IRASET48871.2020.9092280
2. Younes Sahri, Salah Tamalouzt, Sofia Lalouni Belaid Direct Torque Control of DFIG Driven by Wind Turbine System Connected to the Grid 2018 International Conference on Wind Energy and Applications in Algeria (ICWEAA) Year: 2018 | Conference Paper | Publisher: IEEE DOI: 10.1109/ICWEAA.2018.8605083
3. Pandian, Ch. Rami Reddy Cuckoo Search Optimization based MPPT for Integrated DFIG-Wind Energy System B. Srikanth Goud;P. Srinivasa Varma;B. Loveswara Rao;M. Sai Krishna Reddy;A. 2020 International Conference on Decision Aid Sciences and Application (DASA)
4. Year: 2020 | Conference Paper | Publisher: IEEE DOI: 10.1109/DASA51403.2020.9317072
5. Wuyang Su, Bin Liu, Zhen Li, Xuefei Mao, Meng Huang, Guoqing He, Xiangdong Liu Dynamic State Estimation for DFIG Wind Turbine with Stochastic Wind Speed in Power System 2018 IEEE International Symposium on Circuits and Systems (ISCAS) Year: 2018 | Conference Paper | Publisher: IEEE DOI: 10.1109/ISCAS.2018.8351791
6. Youssef Moumani, Abdeslam Jabal Laafou, Abdessalam Ait Madi Modeling and Backstepping Control of DFIG used in Wind Enegry Conversion System 2021 7th International Conference on Optimization and Applications (ICOA) Year: 2021 | Conference Paper | Publisher: IEEE DOI: 10.1109/ICOA51614.2021.9442625
7. Abdeslam Jabal Laafou;Abdessalam Ait Madi;Adnane Addaim Dynamic Control of DFIG used in Wind Power Production, based on PI regulator 2020 IEEE 2nd International Conference on Electronics, Control, Optimization and Computer Science (ICECOCS) Year: 2020 | Conference Paper | Publisher: IEEE DOI: 10.1109/ICECOCS50124.2020.9314563
8. Jitheesh P Gopalan, Binitha Joseph Mampilly, “A Versatile STATCOM for SSR Mitigation and Dynamic Reactive Power Management in DFIG Based Wind Farm Connected to Series Compensated Line 2020 IEEE International Power and Renewable Energy Conference Year: 2020 | Conference Paper | Publisher: IEEE DOI: 10.1109/IPRECON49514.2020.9315202
9. Răzvan Beniugă, Oana Beniugă, Dragoç Machidon Assessment of DFIG wind turbine overvoltage protection system for grid stability 2019 8th International Conference on Modern Power Systems (MPS) Year: 2019 | Conference Paper | Publisher: IEEE DOI: 10.1109/MPS.2019.8759781
10. Jinxin Ouyang;Ting Tang;Jun Yao;Mengyang Li Active Voltage Control for DFIG-Based Wind Farm Integrated Power System by Coordinating Active and Reactive Powers Under Wind Speed Variations IEEE Transactions on Energy Conversion Year: 2019 | Volume: 34, Issue: 3 | Journal Article | Publisher: IEEE

11. Jin Ma, Dawei Zhao, Liangzhong Yao, Minhui Qian, Koji Yamashita, Lingzhi Zhu Analysis on application of a current-source based DFIG wind generator model CSEE Journal of Power and Energy Systems Year: 2018 | Volume: 4, Issue: 3 | Journal Article | Publisher: CSEE DOI: 10.17775/CSEEJPES.2018.00060
12. Subinay Vajpayee, Nihar Ranjan Panda, Prasanajit Behera, Sarat Chandra Swain "Implementation of PLL algorithm in DFIG based wind turbine connected to utility grid 2020 Second International Conference on Inventive Research in Computing Applications" (ICIRCA) Year: 2020 | Conference Paper | Publisher: IEEE DOI: 10.1109/ICIRCA48905.2020.9182961
13. Kamal Ouezgan, Badre Bossoufi, Mohammed Najib Bargach, "DTC Control of DFIG-Generators for Wind Turbines: FPGA Implementation" International Renewable and Sustainable Energy Conference (IRSEC) Year: 2017 | Conference Paper | Publisher: IEEE DOI: 10.1109/IRSEC.2017.8477300
14. Panneer Selvam Manickam, Prakasam Periasamy Tracking the Maximum Wind Power Point using Neuro-Fuzzy Control with DFIG-BESS for Wind Energy System 2018 Conference on Emerging Devices and Smart Systems (ICEDSS) Year: 2018 | Conference Paper | Publisher: IEEE DOI: 10.1109/ICEDSS.2018.8544358
15. Xinglong Wang, Song Han, "Modeling of DFIG based wind farm considering temporal and spatial non-uniformity of wind speed in mountainous region and its applicability analysis" 2017 29th Chinese Control And Decision Conference (CCDC) Year: 2017 | Conference Paper | Publisher: IEEE DOI: 10.1109/CCDC.2017.7978389
16. Preeti Sonkar, O. P. Rahi, "Study of short-term frequency regulation techniques of DFIG Wind turbine" 2017 IEEE International Conference on Power, Control, Signals and Instrumentation Engineering (ICPCSI) Year: 2017 | Conference Paper | Publisher: IEEE DOI: 10.1109/ICPCSI.2017.8392078
17. Xie Hua, Xu Hongyuan, Li Na, "Control strategy of DFIG wind turbine in primary frequency regulation" 2018 13th IEEE Conference on Industrial Electronics and Applications (ICIEA) Year: 2018 | Conference Paper | Publisher: IEEE DOI: 10.1109/ICIEA.2018.8397992
18. Md Aktarujjaman, M. E. Haque, S. Saha, M. Negnevitsky "Impact of DFIG Based Wind Generation on Grid Voltage and Frequency Support" 2020 International Symposium on Power Electronics, Electrical Drives, Automation and Motion (SPEEDAM) Year: 2020 | Conference Paper | Publisher: IEEE DOI: 10.1109/SPEEDAM48782.2020.9161867
19. Anjali V. Deshpande, V. A. Kulkarni Simplified Model of DFIG in Wind Integrated Power System 2019 3rd International Conference on Computing Methodologies and Communication (ICCMC) Year: 2019 | Conference Paper | Publisher: IEEE DOI: 10.1109/ICCMC.2019.8819670